Submitted to the International Europhysics Conference on High Energy Physics HEP99,
Tampere, Finland, July 1999

Diffractive J/ψ Photoproduction

H1 Collaboration

Abstract

Elastic photoproduction of J/ψ mesons is analysed using data from 1996 and 1997 corresponding to an integrated luminosity of about $\int \mathcal{L}\,\mathrm{dt} \sim 21\,\mathrm{pb}^{-1}$. The energy dependence of the total photoproduction cross section is presented and predictions in the framework of perturbative QCD and of a two pomeron model are compared to the data. The t dependence is analysed as a function of $W_{\gamma p}$. A determination of the exchanged trajectory in terms of Regge theory yields a result which is closer to the "hard pomeron" with little shrinkage.

Abstract: 157aj
Parallel sessions: 3, 5
Plenary sessions: 3, 5

Electronic Access: http://www-h1.desy.de/publications/

Introduction

Previous H1 data [1] about elastic photoproduction of J/ψ mesons (that is $ep \to e\, J/\psi\, p$ with the virtuality of the exchanged photon $Q^2\sim\ 0$) have shown features of a diffractive process, such as an exponential t distribution at low t and a transverse polarisation of the J/ψ in agreement with s-channel helicity conservation. However the dependence of the cross section on the photon proton center of mass (cms) energy $W_{\gamma p}$ was found to be much steeper than predicted in diffractive models with one soft pomeron, e.g. by Donnachie and Landshoff [14]. Since then an explanation for this steep rise has been proposed in two different frameworks: in a non perturbative context by introducing a second "hard" pomeron [15] and in a perturbative QCD (pQCD) approach [9, 10]. In pQCD diffractive production of charmonium proceeds via exchange of gluons and the rise of the cross section is related to the increasing gluon density at low values of x observed in deep inelastic scattering at HERA.

We report here on a new analysis using an increased integrated luminosity of about $\int \mathcal{L}\,\mathrm{dt} \sim 21$ pb^{-1}. The data were taken in 1996 and 1997, when HERA was operating with positrons of 27.5 GeV and protons of 820 GeV. The analysis is carried out in the photoproduction limit ($Q^2 \to 0$) and covers a region of $40 < W_{\gamma p} < 150\,$GeV .

Data Analysis

The analysis of the data resembles closely the procedure described in detail in [1] and is only outlined here. Exactly two tracks fitted to the event vertex are required in the central tracking chambers, $20^\circ < \theta < 160^\circ$, one of which has to be identified as a muon in the LAr calorimeter or the muon detector. To reject events in which the proton dissociates counters covering polar angles close to the proton beam ($0.06^\circ < \theta < 0.26^\circ$ and $3^\circ < \theta < 17^\circ$) – the so–called "forward counters" – are utilized. Mass distributions for the selected "forward untagged" data are shown in fig. 1 in the bins of $W_{\gamma p}$ used for the total cross section.

The calculation of the cross section proceeds as follows: after correcting the observed number of events for acceptance, efficiencies, remaining background from proton dissociation and non-resonant background, the ep cross section is obtained. It is converted into a γp cross section assuming factorisation of the ep reaction into emission of photons described by a photon flux followed by a γp interaction. The systematic error was estimated as in previous analyses and the contributions are summarised in table 1.

The cross section for elastic J/ψ meson production as a function of $W_{\gamma p}$ is shown in figure 2 together with previous HERA results [1, 2, 3] and results from fixed target experiments [7, 8]. A fit of the form W^δ to the HERA data between $30 \le W \le 285\,$GeV yields a value of $\delta = 0.81 \pm 0.08$ (including systematic errors). Including fixed target results in the fit yields $\delta = 0.83 \pm 0.05$. This rise with $W_{\gamma p}$ is much steeper than the prediction of the Donnachie-Landshoff model using the soft pomeron only ($\delta = 0.22 - 0.32$).

In figure 3 the two pomeron model [15] is compared with the data. The relative contribution of the "soft" and the "hard" pomerons has been adjusted to the data taking into account interference. The description of the data is improved compared to using only a soft pomeron.

In figure 4 the HERA data are shown with predictions from a leading order pQCD [9, 10] calculation using different gluon density distributions. The important prediction concerns the slope of the cross section while the absolute magnitude depends critically on the mass of the charm quark. Therefore the normalisation of the predictions were adjusted to coincide with the data around $W_{\gamma p} \approx 90$ GeV. The slope of the data is described best using the gluon density CTEQ4M [11] or MRSR2 [13] while GRV-HO [12] is slightly steep.

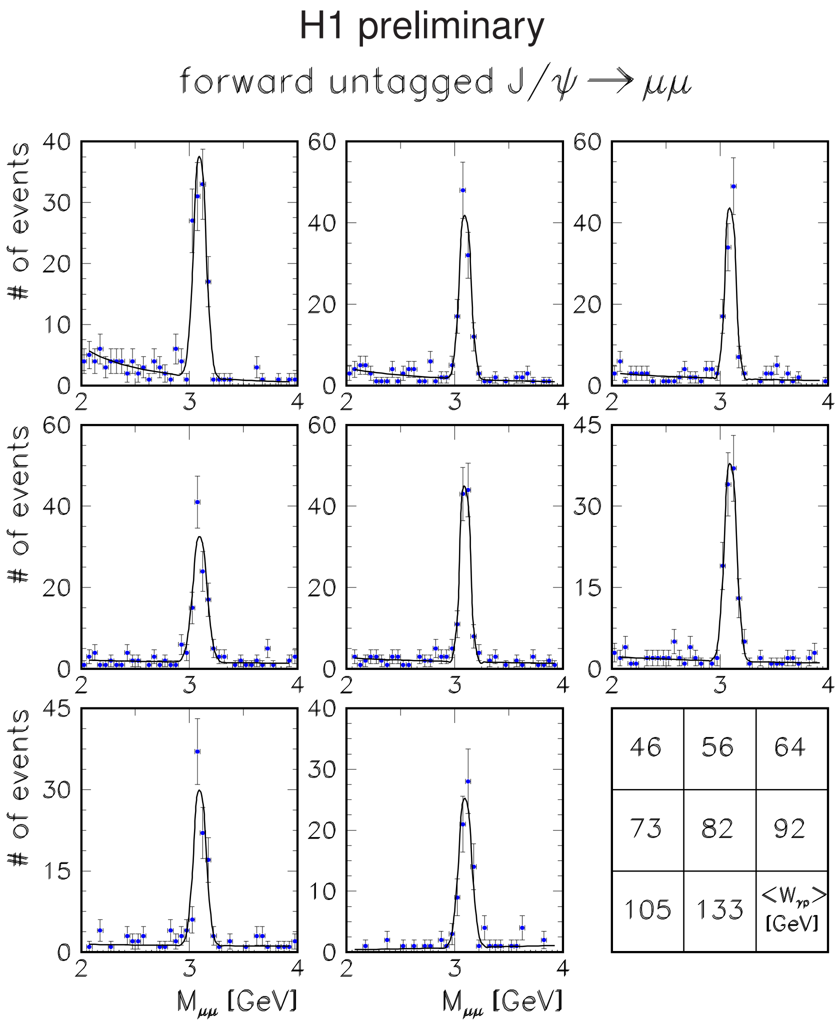

Figure 1: The mass spectra in eight $W_{\gamma p}$ bins for forward untagged data. In the bottom right corner the average values $\langle W_{\gamma p} \rangle$ in each bin are given. From these mass distributions the numbers of J/ψ events are extracted by fits of a Gaussian plus a polynomial for the non-resonant background.

	Source	Amount [%]
1	Track and vertex efficiency	4
2	z-vertex distribution	1
3	Trigger efficiency	4
4	Number of signal events	2
5	$\psi(2S)$ background	1.2
6	Bin center determination	3.3
7	Lepton identification	6.5
8	Forward tagging (*)	5 / 10
9	Luminosity	1.6
10	J/ψ branching ratio	3.2
	Total systematic error (*)	11.4 / 14.3

Table 1: Systematic uncertainties taken into account for the cross section measurement. Items one to six are assumed to be uncorrelated between different $W_{\gamma p}$ bins, whereas the error on the luminosity determination and on the branching ratio are fully correlated in $W_{\gamma p}$. 50% of the errors seven and eight are assumed to be correlated in $W_{\gamma p}$. For the determination of the slope of the $W_{\gamma p}$ dependence only the uncorrelated errors are taken into account. The errors marked by (*) are $W_{\gamma p}$ dependent. The first value is valid for bins one to seven, while the second value is for the highest $W_{\gamma p}$ bin (bin eight).

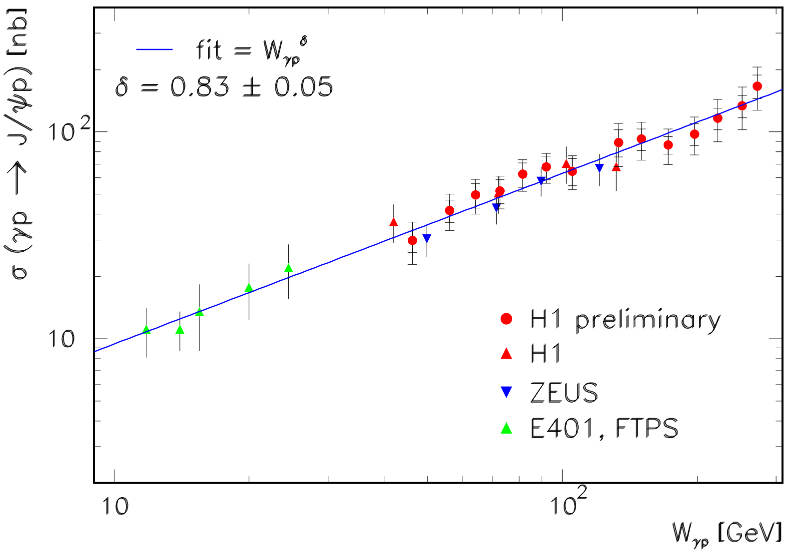

Figure 2: The total photon–proton cross section $\sigma(\gamma p \rightarrow J/\psi p)$ versus $W_{\gamma p}$ resulting from the analysis presented here, from previous HERA results [1, 2, 3] and from low energy measurements [7, 8]. A fit $\propto W_{\gamma p}^{\delta}$ to all data is performed yielding $\delta = 0.83 \pm 0.05$. The inner error bars show the statistical uncertainty, whereas the outer bars give the systematic and the statistical errors added in quadrature.

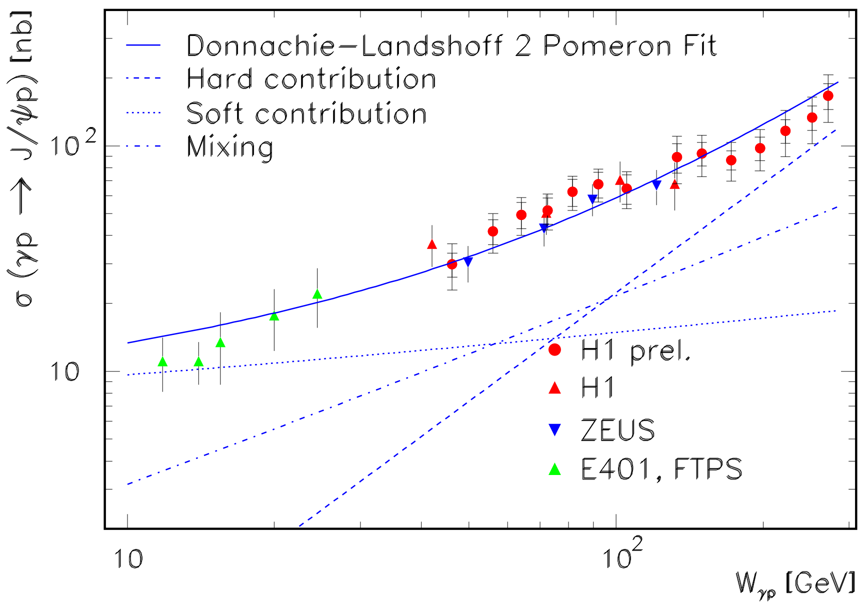

Figure 3: The total photon–proton cross section $\sigma(\gamma p \to J/\psi p)$ versus $W_{\gamma p}$ for this analysis, previous HERA results and low energy measurements. A fit according to the two-pomeron model by Donnachie and Landshoff is performed to all data adjusting only the contributions of the two pomerons. The dashed curves represent the *soft* and the *hard* pomeron contribution as well as their mixing.

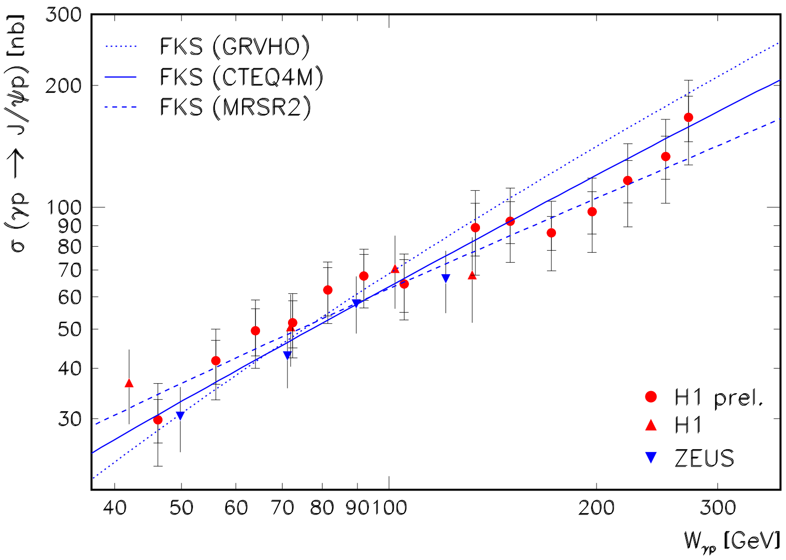

Figure 4: The total photon–proton cross section $\sigma(\gamma p \to J/\psi p)$ versus $W_{\gamma p}$ for this analysis and previous HERA results. The data are shown together with predictions by Frankfurt et al. [10] using different parameterisations of the gluon density in the proton. Note that the normalisation of the curves has been adjusted to the data!

The t Distribution for Elastic J/ψ Production

The momentum transfer t at the proton vertex can be approximated by the transverse momentum of the J/ψ, $-p_t^2$, for photoproduction. The differential cross section can be fitted by an exponential $exp(-b\,|t|)$ for low values of t. The t distribution is shown in fig. 5 for the data of this analysis integrated over $W_{\gamma p}$. A value $b = 4.2 \pm 0.2 \pm 0.6$ is derived for $|t| \leq 0.8$ GeV^2.

The soft pomeron model [14] predicts a logarithmic increase of the b slope with $W_{\gamma p}$:

$$b = b_0 + 4\alpha' \ln W_{\gamma p}/W_0,$$

with $\alpha' = 0.25$ (shrinkage). The hard pomeron shows much less shrinkage: $\alpha' = 0.1$ [15]. In predictions derived in the context of pQCD there is also little or no shrinkage. To evaluate the b slope as a function of $W_{\gamma p}$ the data are analysed in five $W_{\gamma p}$ bins shown in fig. 6. Fits to the distributions of $|t|$ below $0.8\,\mathrm{GeV}^2$ are performed. The resulting values for b are indicated in the figures 6. They are also shown in figures 7 and 8 as a function of $W_{\gamma p}$. Fig. 8 includes previous HERA results and one result from a fixed target experiment[1]. A fit to all data allowing for shrinkage yields:

$$b = (4.5 \pm 0.2) \; + \; 4 \cdot (0.18 \pm 0.09) \cdot \ln(\frac{W_{\gamma p}}{90 \text{ GeV}})\,[\,\mathrm{GeV}^{-2}].$$

Assuming no $W_{\gamma p}$ dependence the average b is:

$$b = 4.3 \pm 0.2\,[\,\mathrm{GeV}^{-2}].$$

The data are clearly compatible with being independent of $W_{\gamma p}$, shrinkage can however not be excluded in view of the errors.

[1] The data points from [8] were re-fitted with one exponential.

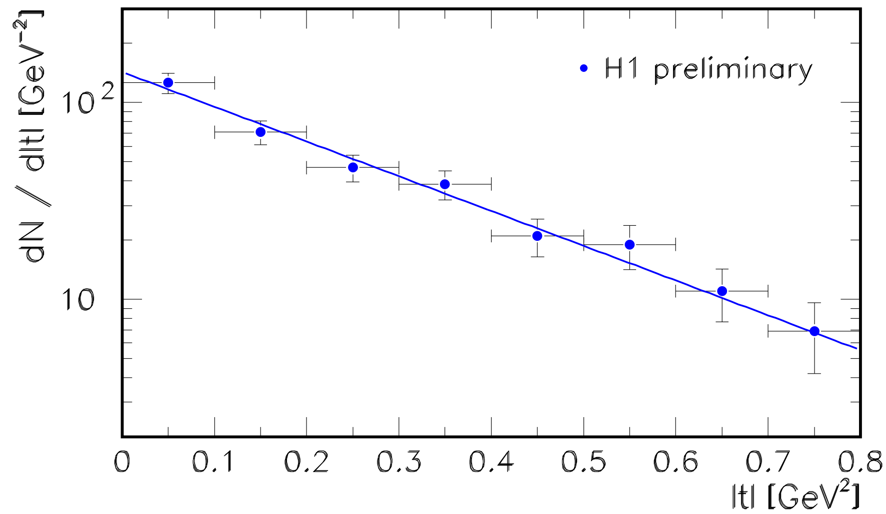

Figure 5: The corrected number of elastically scattered events $dN/d|t|$ as a function of $|t|$ for the energy region $40 < W_{\gamma p} < 150$ GeV together with a fit to the data of the form $dN/d|t| \propto exp(-b\,|t|)$.

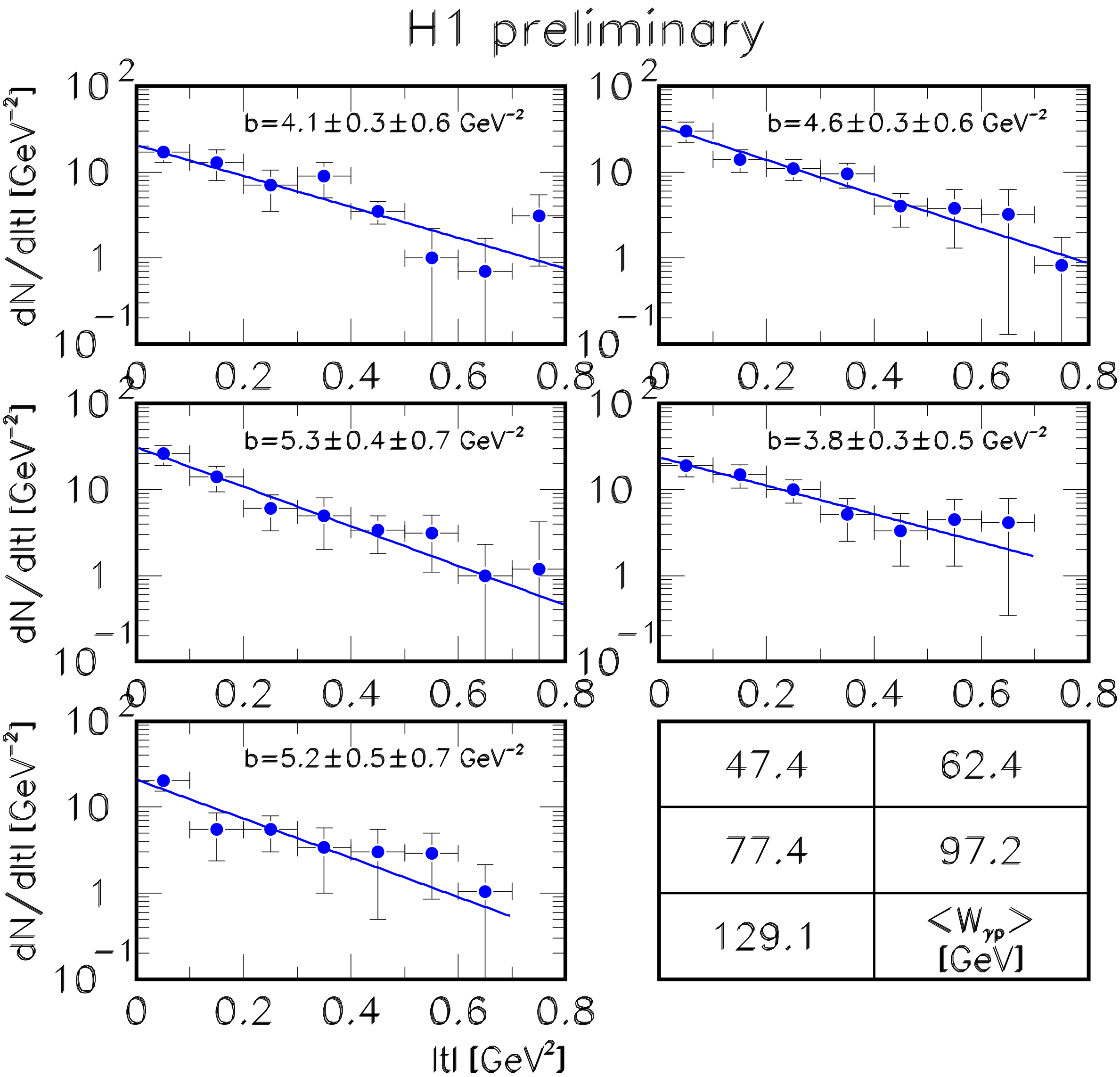

Figure 6: The corrected numbers of events $dN/d|t|$ as functions of $|t|$ for five bins in $W_{\gamma p}$ together with fits to the data of the form $dN/d|t| \propto exp(-b\,|t|)$.The resulting b is indicated. In the right bottom corner the average $\langle W_{\gamma p}\rangle$ values for the chosen bins are given.

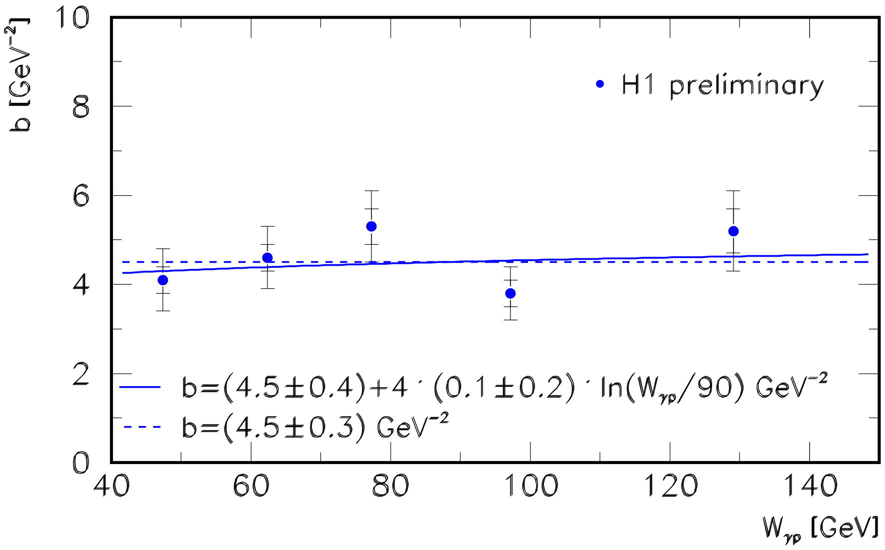

Figure 7: The result for b in the five $W_{\gamma p}$ bins from this analysis alone. The inner error bars are the statistical errors only, while the outer bars are the statistical and the systematic errors added in quadrature. In addition two different fit results are shown, assuming the presence (full line) respectively the absence (dashed line) of shrinkage.

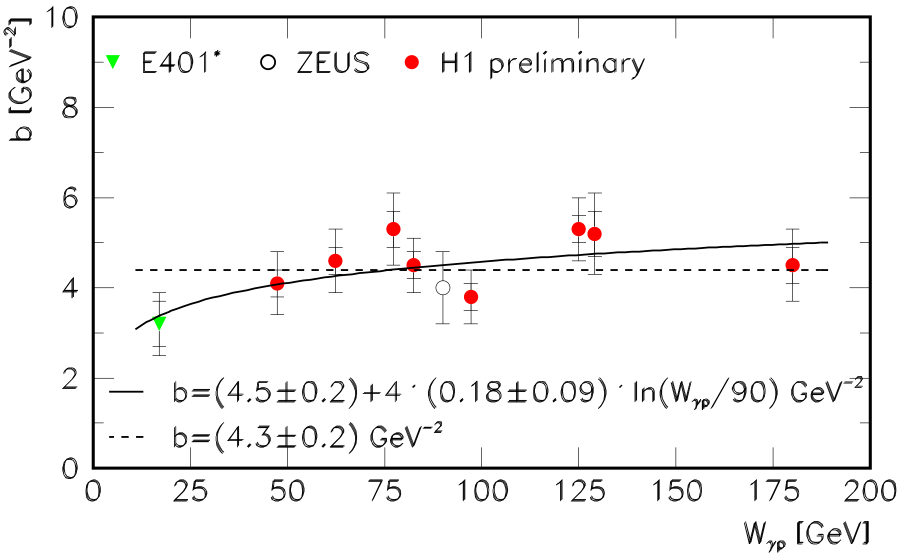

Figure 8: The result for b in the five $W_{\gamma p}$ bins from this analysis together with previous H1 measurements as well as a modified E401 value. The inner error bars are the statistical errors only, while the outer bars are the statistical and the systematic errors added in quadrature. In addition two different fit results are shown, assuming the presence (full line) respectively the absence (dashed line) of shrinkage.

Regge Trajectory for Elastic J/ψ Production

A more direct way of determining the properties of the exchange in diffractive J/ψ production is proposed in [16]. The data are divided into five t bins and 6 bins of $W_{\gamma p}$. The mass distributions in these bins are shown in fig. 9. The bin sizes have been adjusted so that the number of events is roughly equal. In fig. 10 the differential cross section is shown as a function of $W_{\gamma p}$ for these t bins . The data are fitted with a function:

$$\frac{d\sigma}{dt_i}(W_{\gamma p}) = N_i \cdot (W_{\gamma p}/90\ \text{GeV})^{4\alpha(t_i)-4}$$

using N_i and $\alpha(t_i)$ as free parameters. The resulting values of $\alpha(t_i)$ are then fitted to the form $\alpha_0 + \alpha' \cdot t$ where α_0 and α' are free parameters. The result is:

$$\alpha(t) = (1.26 \pm 0.05) + (0.05 \pm 0.15) \cdot t.$$

This fit result is shown in fig. 11 as a band reflecting the 1s.d. contour taking into account correlations. The result favours little shrinkage (compare the slope of the "soft" and "hard" pomerons which are also indicated in the figure). Also shown is a prediction for a pomeron derived in the context of the BFKL equation [17]. The predictions of the fit and the various pomerons are also shown in fig. 10. Also here one sees that the data come closest to the "hard" Donnachie-Landshoff pomeron or the "BFKL pomeron".

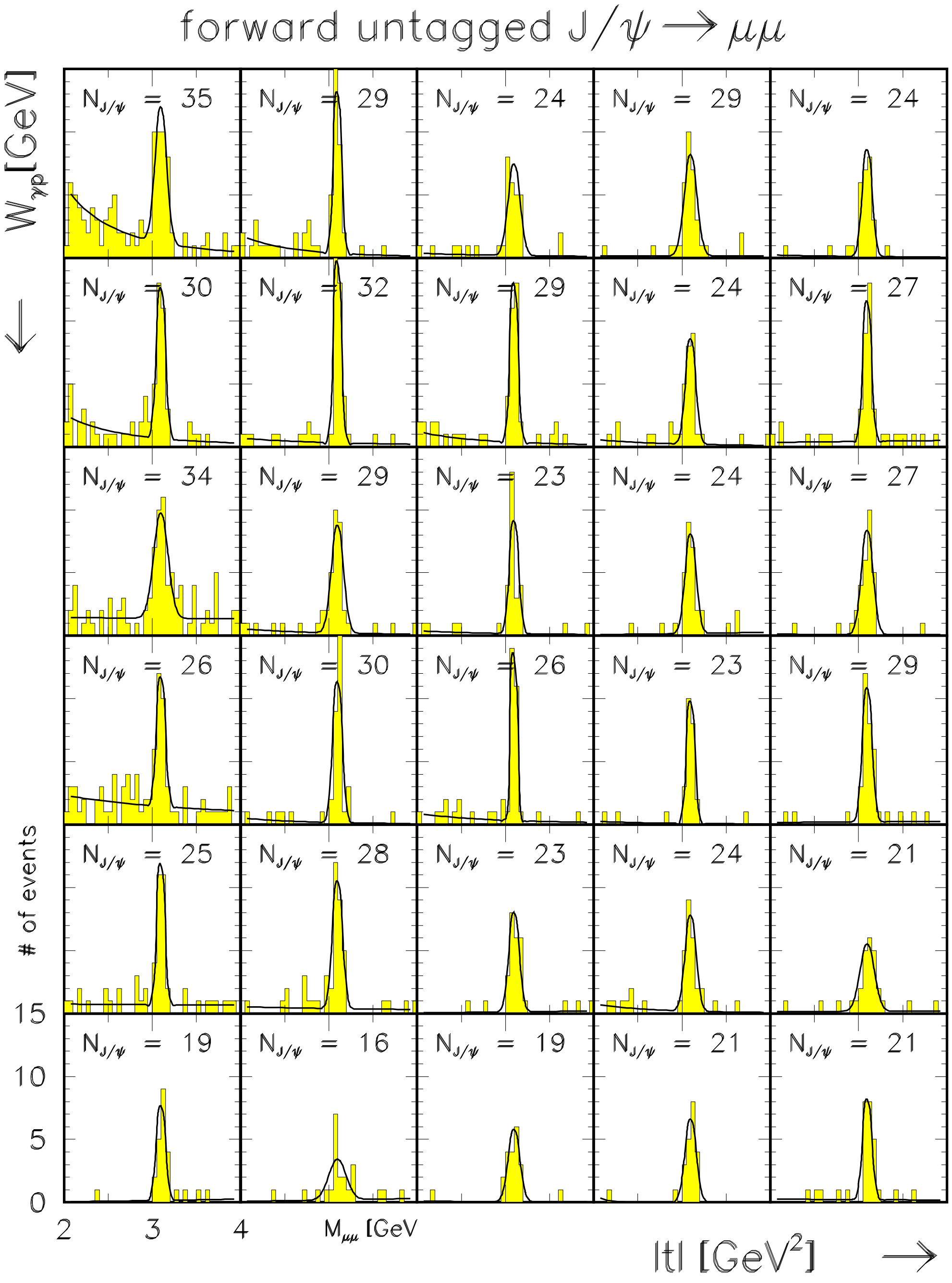

Figure 9: Forward untagged $J/\psi \to \mu\mu$ signals in the $W_{\gamma p} - |t|$ plane. Shown are the invariant mass distributions between $2 \leq M_{\mu\mu} \leq 4$ GeV in bins of $W_{\gamma p}$ and $|t|$, with $40 \leq W_{\gamma p} \leq 150$ GeV and $0 \leq |t| \leq 1.5$ GeV^2. The bins are chosen such that the number of signal events is roughly the same everywhere. The number of J/ψ mesons is obtained by a fit of a Gaussian for the resonance plus a polynomial for the non-resonant background and given in each bin.

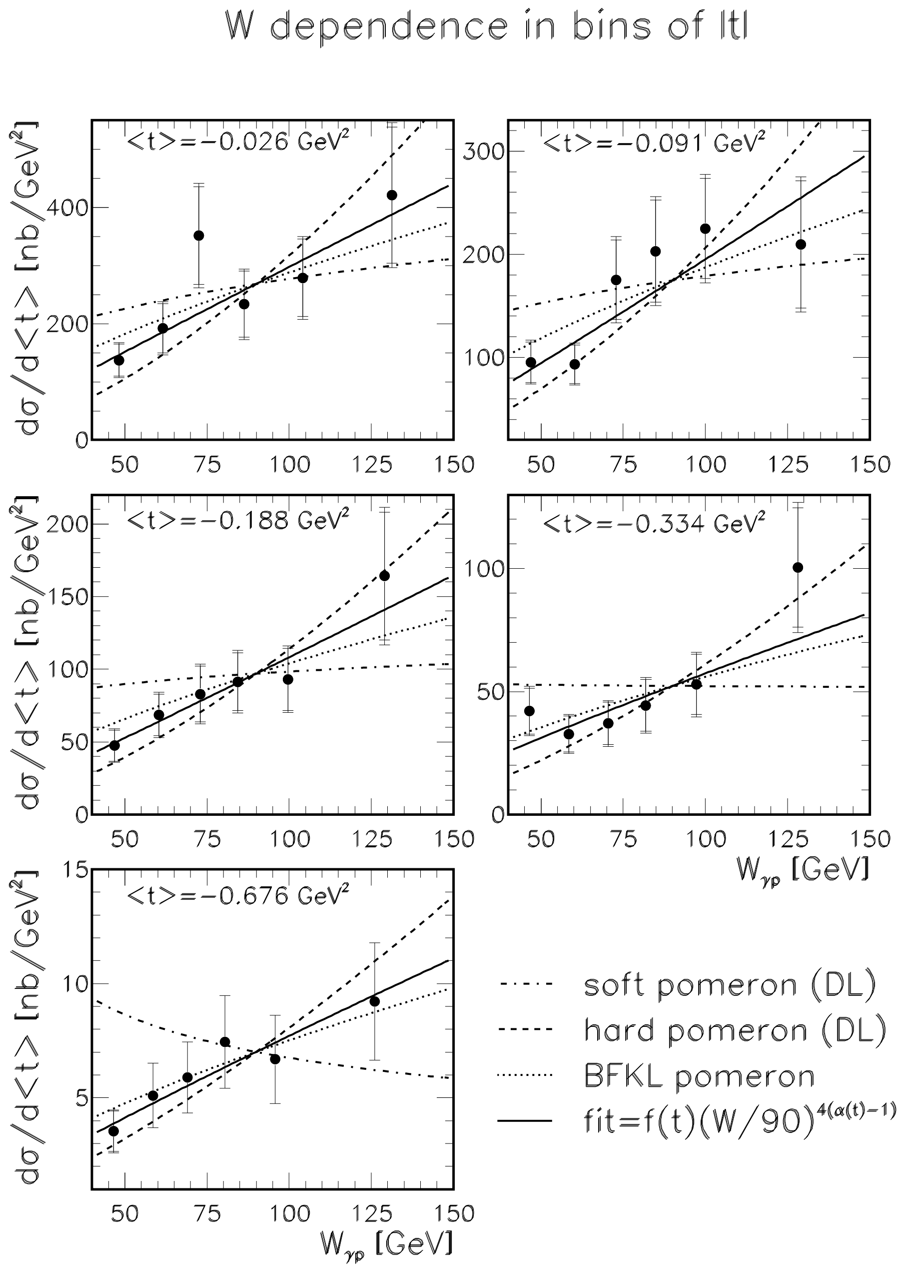

Figure 10: The differential γp cross section $d\sigma/dt$ as a function of $W_{\gamma p}$ in five bins of t together with a fit of the form $\frac{d\sigma}{dt} = N \cdot (W_{\gamma p}/90\ \text{GeV})^{4\alpha(t)-4}$. The average t values are indicated in the plots. The predictions of the soft and hard pomeron are shown as dash-dotted and dashed lines, respectively. The prediction of the BFKL pomeron is indicated as a dotted line.

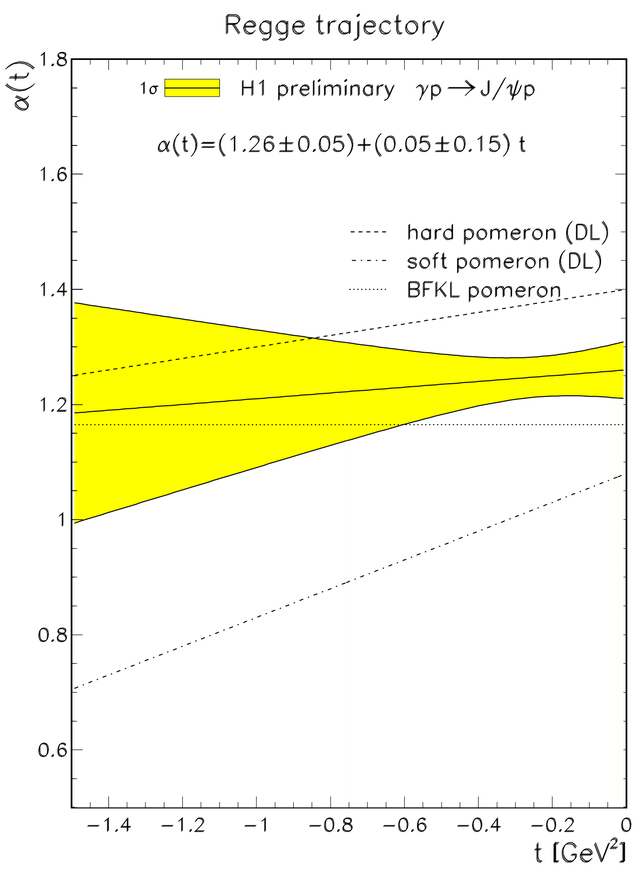

Figure 11: The measured Regge trajectory $\alpha(t) = \alpha_0 + \alpha' \cdot t$ for the process $\gamma p \to J/\psi\, p$. The data are given by the 1 s.d. band. The resulting numbers are indicated in the figure. Also shown are the soft and the hard Donnachie-Landshoff pomeron trajectories [15] and a pomeron derived from the BFKL equation [17].

Summary and Conclusions

In the present analysis improved results on the energy dependence of the total photoproduction cross section, on the t dependence and on the energy dependence of the t slope parameter are derived. A determination of the Regge trajectory for J/ψ production is carried out. These results shed further light on the question about the mechanism of diffractive J/ψ photoproduction at HERA.

- The measured $W_{\gamma p}$ dependence of the total γp cross section over the entire accessible energy range including data from previous HERA and fixed target experiments ($15 \leq W_{\gamma p} \leq 285$ GeV):

$$\sigma_{\gamma p} \propto W_{\gamma p}^{0.83 \pm 0.05} \tag{1}$$

  is significantly steeper than predicted by *soft* pomeron exchange ($\sigma_{\gamma p} \propto W_{\gamma p}^{0.22-0.32}$), but it is in fair agreement with a new approach in the context of Regge theory, the two–pomeron model which assumes the exchange of two pomeron trajectories, a *soft* and a *hard* pomeron. A perturbative QCD calculation by Frankfurt et al. in which the rise of the cross section reflects the increasing gluon density in the proton with decreasing momentum fraction x gives also a good description of the HERA data.

- Results for the elastic slope parameter b are:

$$b = 4.2 \pm 0.2 \pm 0.6 \text{ GeV}^{-2} \quad \text{for} \quad 40 \leq W_{\gamma p} \leq 150 \text{ GeV} \quad (\langle W_{\gamma p} \rangle = 89.4 \text{ GeV})\,. \tag{2}$$

  b has also been determined in five bins of $W_{\gamma p}$. No significant energy dependence can be seen from this measurement alone. This is also true for the combination with previous HERA data and low energy measurements:

$$b = (4.5 \pm 0.2) + 4 \cdot (0.18 \pm 0.09) \cdot ln \frac{W_{\gamma p}}{90 \text{ GeV}} \text{ GeV}^{-2}\,. \tag{3}$$

- The directly measured Regge trajectory exchanged in elastic J/ψ photoproduction at HERA favours the absence of shrinkage of the diffractive peak, but the data are not yet precise enough to allow a final judgement on this question. The intercept and the slope of the measured trajectory are

$$\alpha(t) = (1.26 \pm 0.05) + (0.05 \pm 0.15) \text{ GeV}^{-2} \cdot t\,, \tag{4}$$

  thus lying in between the two pomeron trajectories of Donnachie and Landshoff.

Finally, it can be stated that a description of the data is possible in perturbative QCD using current gluon densities as well as with results from Regge theory under the assumption of a second *hard* pomeron. Based on the energy dependence of the cross section as well as the energy independence of the slope parameter, a pure *soft* production mechanism can be ruled out.

References

[1] H1 Collaboration, S. Aid et al., Nucl. Phys. **B472** (1996) 3.

[2] ZEUS Collaboration, J. Breitweg et al., Z. Phys. **C75** (1997) 215.

[3] H1 Collaboration, C. Adloff et al., *Elastic Production of J/ψ Mesons in Photoproduction and at High Q^2 at HERA*, contributed paper 242 to HEP 1997, Jerusalem.

[4] H1 Collaboration, C. Adloff et al., *Shrinkage in Exclusive J/ψ Photoproduction*, contributed paper 572 to ICHEP 1998, Vancouver.

[5] H1 Collaboration, C. Adloff et al., *Energy Dependence of the Cross-Section for the Exclusive Photo-Production of J/ψ Mesons at HERA*, contributed paper 572 to ICHEP 1998, Vancouver.

[6] H1 Collaboration, C. Adloff et al., *Charmonium Production in Deep Inelastic Scattering at HERA*, Europ. Journal f. Phys. (1999).

[7] E516 Collaboration, B.H. Denby et al., Phys. Rev. Lett. **52** (1984) 795.

[8] E401 Collaboration, M. Binkley et al., Phys. Rev. Lett. **48** (1982) 73.

[9] L. Frankfurt, W. Koepf and M. Strikman, Phys. Rev. **D54** (1996) 319.

[10] L. Frankfurt, W. Koepf and M. Strikman, Phys. Rev. **D57** (1998) 512.

[11] H. L. Lai et al., Phys. Rev. **D55** (1997) 1280.

[12] M. Glück, E. Reya and A. Vogt, Z. Phys. **C67** (1995) 433.

[13] A. D. Martin, R. G. Roberts and W. J. Stirling, Phys. Lett. **B387** (1996) 419.

[14] A. Donnachie and P.V. Landshoff, Phys. Lett. **B348** (1995) 213.

[15] A. Donnachie, P. V. Landshoff, hep-ph/9806344 (1998).

[16] A. Levy, hep-ph/9712519 (1997).

[17] S.J. Brodsky et al., SLAC-PUB-8037, hep-ph/9901229 (1999).